Virology 416 (2011) 16–25

Contents lists available at ScienceDirect

Virology

journal homepage: www.elsevier.com/locate/yviro

The protease-sensitive loop of the vesicular stomatitis virus matrix protein is involved in virus assembly and protein translation

Chad E. Mire [1], Michael A. Whitt *

Department of Microbiology, Immunology and Biochemistry, University of Tennessee Health Science Center, 858 Madison Avenue, Memphis, TN 38163, USA

ARTICLE INFO

Article history:
Received 23 January 2011
Returned to author for revision
24 February 2011
Accepted 25 April 2011
Available online 18 May 2011

Keywords:
Vesicular stomatitis virus
Matrix protein
Virus assembly
Virus protein translation

ABSTRACT

To study the contribution of the protease-sensitive loop of the VSV M protein in virus assembly we recovered recombinant VSV (rVSV) with mutations in this region and examined virus replication. Mutations in the highly conserved LXD motif (aa 123–125) resulted in reduced virion budding, reduced virus titers and enhanced M protein exchange with M-ribonucleocapsid complexes (M-RNPs), suggesting that the mutant M proteins were less tightly associated with RNP *skeletons*. In addition, viral protein synthesis began to decrease at 4 h post-infection (hpi) and was reduced by ~80% at 8 hpi for the mutant rVSV-D125A. The reduced protein synthesis was not due to decreased VSV replication or transcription; however, translation of a reporter gene with an EMCV IRES was not reduced, suggesting that cap-dependent, but not cap-independent translation initiation was affected in rVSV-D125A infected cells. These results indicate that the LXD motif is involved in both virus assembly and VSV protein translation.

Introduction

Vesicular stomatitis virus (VSV) is a simple, enveloped, non-segmented negative-strand RNA virus that has served as a good model to study virus replication and assembly. There are two major serotypes of VSV found in the United States, VSV-Indiana (VSV-Ind) and VSV-New Jersey (VSV-NJ), both of which are part of a larger group of related vesiculoviruses that belong to the family *Rhabdoviridae*. The genome of VSV encodes the nucleocapsid (N) protein, the phosphoprotein (P), the matrix (M) protein, the glycoprotein (G), and the large (L) polymerase protein. The viral genomic RNA is encapsidated by the N protein and is associated with the RNA-dependent RNA polymerase (RdRp), which consists of a complex of the L and P proteins. Together, the encapsidated genome and associated RdRp make up the ribonucleoprotein particle (RNP). During virus assembly at the plasma membrane, RNPs localize to membrane microdomains containing G protein to form budding sites (Brown and Lyles, 2003a, 2003b). The M protein, which is found in both the cytoplasm and associated with the inner leaflet of the plasma membrane, is recruited into budding sites (Swinteck and Lyles, 2008) where it condenses the RNP into a tightly packed helix called the *skeleton* (Newcomb and Brown, 1981; Newcomb et al., 1982). Recently, cryo-electron microscopy (cryo-EM) of VSV-Ind virions revealed that the *skeleton* is a left-handed helix with M on the outside of the RNP anchoring it to the viral membrane (Ge et al., 2010). Surrounding the *skeleton* is the viral envelope derived from the host cell plasma membrane with G protein trimers protruding from the surface. The M protein of VSV plays a key role in virus assembly by condensing the RNP and it also contributes to the release of virions by budding from the cell surface (Chong and Rose, 1994; Harty et al., 2001; Jayakar et al., 2000). The M protein is also responsible for inducing the cytopathic effects (CPE) characteristic of a VSV infection, which include disruption of cytoskeletal organization, inhibition of host mRNA expression, inhibition of host translation, impeding nucleocytoplasmic transport, and induction of apoptosis (Ahmed and Lyles, 1998; Ahmed et al., 2003; Connor and Lyles, 2005; Faria et al., 2005; Petersen et al., 2000).

Biochemical studies suggest that an exposed protease-sensitive loop (amino acids 120-PAVLADQGQP-129) in M may be important for assembly of virions. Cleavage of this region in the M protein from VSV-Ind with the protease thermolysin resulted in an M protein that no longer self-associates (Gaudier et al., 2001, 2002). M self-association has been implicated in condensation of RNPs (Gaudin et al., 1995; Newcomb et al., 1982), which is critical for the formation of the bullet-shaped particles characteristic of rhabdovirus virions (Lyles et al., 1996; Mebatsion et al., 1999). The recent cryo-EM analysis of VSV virions led to a model of virion assembly where the loop region was important for M-M interactions between consecutive helical turns of the RNP (Ge et al., 2010). This was supported by the determination of the crystal structure of the M protein from VSV-NJ, which included amino acids 122–127 of the loop, and which showed that the N-terminal region of an adjacent M monomer interacted with the loop region in self-assembled M oligomers (Graham et al., 2008).

* Corresponding author. Fax: +1 901 448 7360.
E-mail address: mwhitt@uthsc.edu (M.A. Whitt).
[1] Current address: University of Texas Medical Branch, Department of Microbiology and Immunology, Galveston National Laboratory, 301 University Boulevard, Galveston, TX 77555-0610, USA.

0042-6822/$ – see front matter © 2011 Elsevier Inc. All rights reserved.
doi:10.1016/j.virol.2011.04.013

To understand the role of the protease-sensitive loop of VSV-Ind M in virus assembly, Connor and Lyles (Connor et al., 2006) mutated the hydrophobic core of the loop from AVLA to KDQQ. Interestingly, the effect on virus assembly was minor, but the mutations resulted in reduced viral protein synthesis. Here, we report on the effect of additional mutations within the loop region on viral protein synthesis and VSV-Ind assembly. Characterization of the mutants revealed no effect on the cellular distribution or the in vitro budding activity of the M mutants compared to wild-type M protein (Mwt); however, attempts to recover recombinant virus encoding some of the mutants were unsuccessful. For those that were recovered, the viruses grew to lower titers and produced less total virus, indicating that the mutations in the loop may have affected virus assembly. Metabolic labeling studies with rVSV-infected cells revealed that one of the mutants (D125A) had reduced levels of viral protein synthesis beginning at 4 hpi, similar to that reported previously by Connor et al. (2006). The reduced protein synthesis for our mutant was not due to reduced genome replication or mRNA transcription. These results suggest that the protease-sensitive loop in VSV-Ind M is important for VSV assembly and that it also positively regulates translation by an unknown mechanism. Sequence analysis of this region identified a conserved LXD motif (residues 123–125 for VSV-Ind M) that is found in the matrix proteins of other vesiculoviruses, suggesting that the LXD sequence may represent an interaction motif important for reversible assembly–disassembly reactions, such as is needed during virus assembly and uncoating.

Results

Recovery and characterization of rVSVs with M loop mutations

Previous studies by Gaudier et al. (2001, 2002) identified a protease-sensitive loop in the M protein of VSV-Ind that, when digested with thermolysin, prevented the self-association of M and allowed M protein to be crystallized. Using coordinates from the M crystal structures of VSV-Ind and VSV-NJ (Graham et al., 2008), this region is clearly seen as a loop (Fig. 1A) extending from the main framework of the M structure. Alignment of the putative loop regions from several different vesiculovirus M proteins revealed that the leucine and aspartate residues within this region are conserved (Fig. 1A). Amino acids that were not present in the crystal structure of M-Ind are shown in lower case as are the residues released after thermolysin cleavage. Based on the vesiculovirus M alignments (Fig. 1A), we constructed a series of mutations (Fig. 1B) to determine whether the loop itself (Δ Loop), the size of the loop (2X Loop), or specific amino acids within the loop were involved in the assembly and budding of VSV. All of the constructs included a C-terminal tetracysteine (Lumio) tag, which we have shown does not affect M protein localization, budding activity, or uncoating when assembled into virus particles (Mire et al., 2009, 2010).

To examine the effect of the mutations on the cellular distribution and function of M, we transiently expressed the proteins in BHK cells and compared them to wild-type M protein (Mwt) by immunofluorescence microscopy (IF) and by an in vitro budding assay. There were no discernable differences in the intracellular distributions of the M loop mutants after staining with a monoclonal anti-M antibody (23H12) conjugated to Alexa-546 (Fig. 1C). The loop mutants (only D125A is shown) also had wild-type budding activity (Fig. 1D).

To determine if the M loop mutants could support virus assembly we replaced the Mwt gene in the viral genome with those encoding the loop mutants (Fig. 1B). In contrast to the results of the in vitro budding assay where all of the mutants showed wild-type budding activity, only viruses with single amino acid substitutions (D125A, L123A, and L123S) were recovered. Multiple attempts ($n=6$) to recover the other viruses were unsuccessful. One-step growth curves revealed that the L123A, L123S, and D125A mutant viruses grew more slowly, produced small plaques, and generated final titers that were approximately one-log less than rVSV-wt (Fig. 2A). Because all three

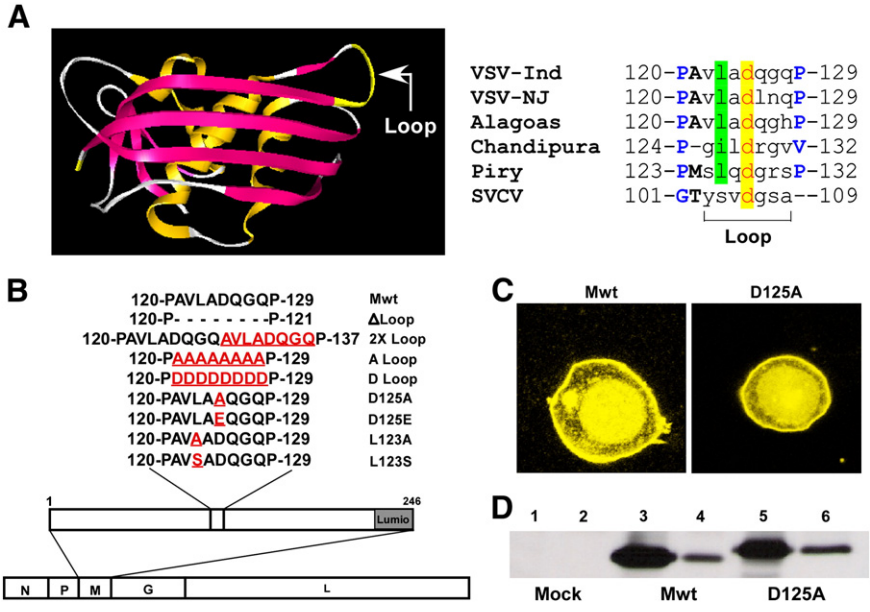

Fig. 1. Identification of a conserved LXD motif and characterization of M protein loop mutants. (A) Location of the protease-sensitive loop in VSV M protein is shown. The image was generated using coordinates from the VSV-Ind M crystal structure (MMDB ID: 50117; PDB ID: 1LG7 (Gaudier et al., 2002)) and viewed in 3D Molecule Viewer. The loop regions from 6 different vesiculoviruses were aligned using Clustal W and the location of the conserved aspartate residue (red font with yellow highlight) and semiconserved leucine/isoleucine (green highlight) are shown. (B) Schematic of mutations made in the protease-sensitive loop region of M and their location within rVSV genomes. The residues in red and underlined are either mutated to the amino acids shown, or are added (2X Loop). The Δ Loop mutant has all amino acids between the two proline residues at positions 121 and 129 deleted. All constructs have a tetracysteine Lumio tag at the C-terminus. (C) Transient expression of Mwt and the D125A loop mutant in BHK-21 cells stained using an anti-M monoclonal antibody conjugated to Alexa-546 and examined by LSCM. The images shown are 1 μm optical sections through the middle of the cell. (D) Budding assay showing intracellular protein expression (odd numbered lanes) and M protein budded into the supernatant in mock transfected (lane 2), Mwt (lane 4), and D125A (lane 6) transfected cells.

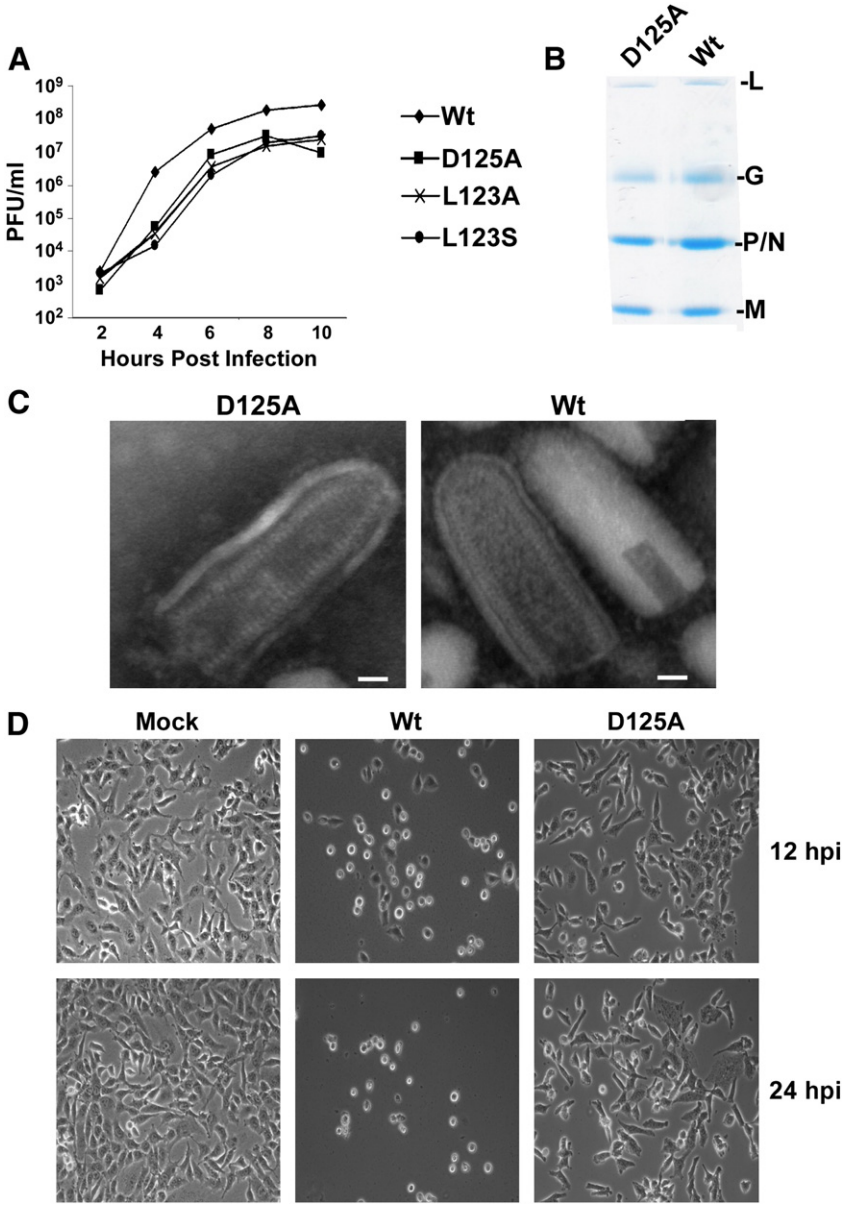

Fig. 2. Characterization of rVSV-M loop mutants. (A) One-step growth curves of rVSV-M mutants and rVSV-wt in BHK-21 cells. Average titers from the experiment performed in triplicate are shown. (B) Coomassie-blue stained SDS-polyacyrlamide gel of 10^7 PFU of rVSV-D125A (lane 1) and rVSV-wt (lane 2). (C) Transmission electron micrographs of purified rVSV-D125A (D125A) and rVSV-wt (Wt) virions at 130,000× magnification. Bar represents 20 nm. (D) Phase-contrast images of BHK-21 cells infected with rVSV-wt (Wt) or rVSV-D125A (D125A) at 12 and 24 hpi.

mutants gave similar results, we focused on characterization of the D125A mutant since the aspartate residue of the LXD motif was the most highly conserved between the vesiculoviruses M proteins (Fig. 1A).

To determine if the reduced infectivity was due to differences in the amount of G or M protein incorporated into virions we assessed the relative infectivity of the viruses released in the one-step growth curve. Proteins from 10^7 plaque forming units (PFU) of the rVSV-D125A and rVSV-wt virions were separated by SDS-PAGE and stained using Coomassie-blue (Fig. 2B). The protein compositions from equivalent amounts of infectious virus were similar indicating that the reduced infectivity for rVSV-D125A was due to fewer virions being released from infected cells and not because less G or M protein was present, or because the virions were inherently less infectious. We then compared the morphology of purified virions by negative-stain transmission electron microscopy (TEM). The morphologies of the rVSV-D125A loop mutant and rVSV-wt (Wt) were similar with bullet-shaped virions and helically condensed RNPs (Fig. 2C), suggesting that the reduced titers were not due to gross changes in virion structure.

In addition to the reduced titers, another notable difference between the D125A mutant and rVSV-wt was that infection with rVSV-D125A did not cause cell rounding (Fig. 2D). A similar phenotype was observed by others (Connor et al., 2006) for a different type of loop mutant in which the hydrophobic amino acids (121-AVLA-124) were changed to charged and polar residues (121-DKQQ-124; rVSV-ΦM). Infection of MDCK cells with rVSV-ΦM did not result in typical VSV-induced cell rounding. However, cell rounding with rVSV-ΦM was observed in BHK infected cells (Connor et al., 2006). In contrast, BHK cells infected with rVSV-D125A did not show typical VSV CPE (Fig. 2D). The cells retained their fibroblast-like appearance, but the cells appeared to be in a quiescent state and did not grow (compare the number of mock-infected versus D125A-infected cells at 24 h post-infection (hpi) in Fig. 2D).

rVSV loop mutants have defects in assembly

To determine if the reduced titers for rVSV-D125A were due to defects in the release of virions from infected cells when compared to rVSV-wt infected cells, we performed virus budding assays. BHK cells were infected and pulse-labeled with ^{35}S-Met at 3 hpi for 1 h. Released virus was purified from the cell supernatants and cell lysates were prepared immediately after the pulse and the labeled proteins were analyzed by SDS-PAGE. To determine the efficiency of virus budding we compared the amount of labeled N protein in virus particles released in the supernatant to the amount of N protein in cell lysates. For rVSV-D125A infected cells only 1.3% of labeled N protein was released from cells at this time point, while approximately 12% of labeled N protein was released from rVSV-wt infected cells (Fig. 3A).

To determine if the reduced level of virus budding could be rescued by Mwt we co-infected cells with rVSV-wt and rVSV-D125A. To eliminate possible variability in the rate of virus internalization between the two viruses and to ensure that the cells were infected simultaneously, we synchronized infection by allowing virus to endocytose in the presence of ammonium chloride and then washed out the drug to initiate infection. In other studies we have found that the number of cells that become co-infected versus singly infected was much higher when fusion is synchronized by ammonium chloride washout as compared to normal (non-synchronized) infection conditions (Watanabe, Mire, and Whitt, unpublished data). For these

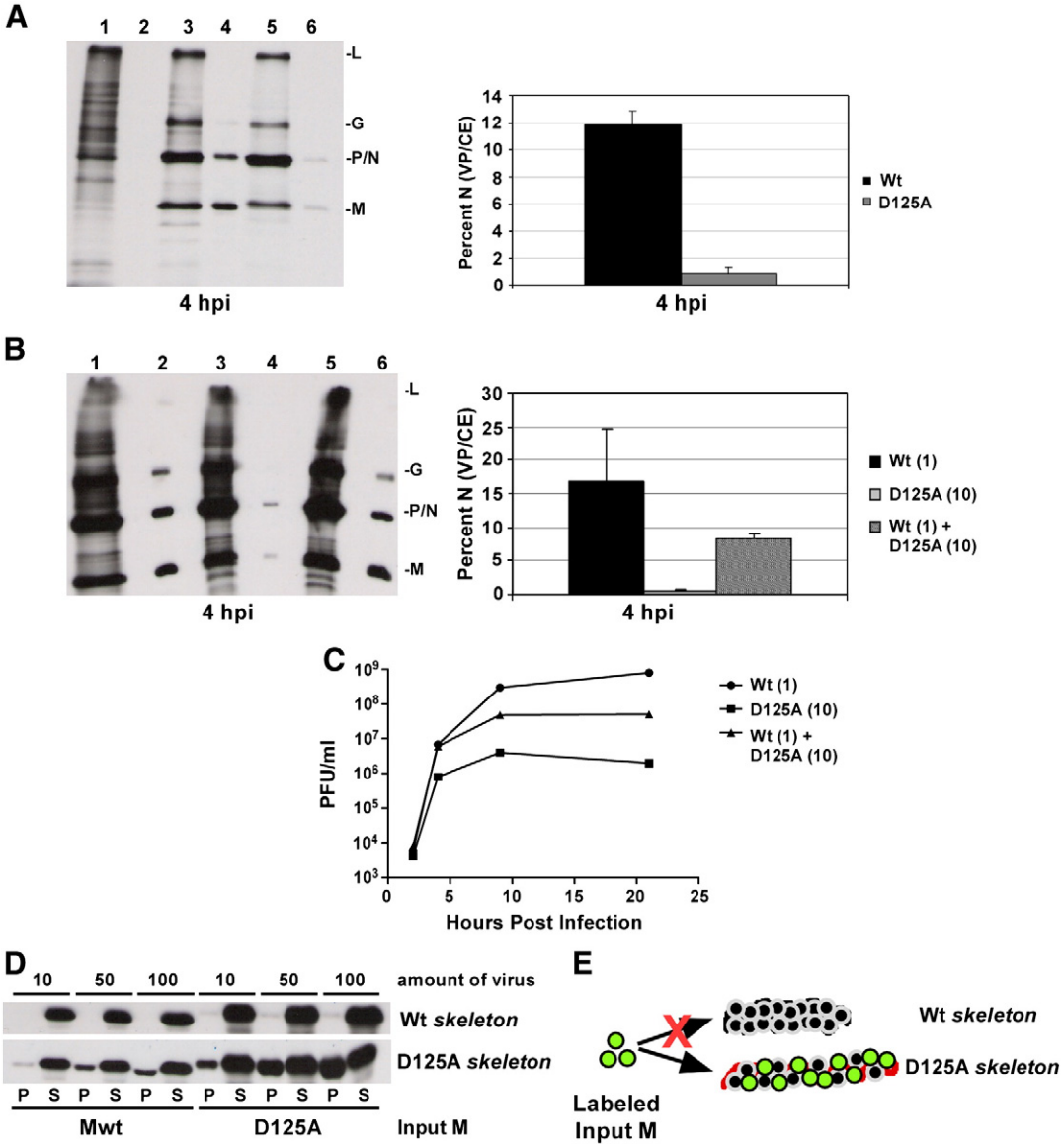

Fig. 3. Analysis of infectious virus production and M-*skeleton* exchange for rVSV-D125A. (A) Amount of viral protein synthesis in cells (odd numbered lanes) and released virus (even numbered lanes) after mock infection (lanes 1 and 2), or after infection with rVSV-wt (lanes 3 and 4) or rVSV-D125A (lanes 5 and 6). Cells were pulse-labeled with ^{35}S-methionine for 1 h at 3 hpi. Labeled virus released in the culture supernatant was harvested by centrifugation and cell lysates were prepared. Samples were analyzed by SDS-PAGE and fluorography and the ratio of virus (N protein) released in the supernatant (VP, viral pellet) to the amount of N protein in cell lysates (CE, cell extract) was determined after quantification by phosphorimaging. (B) Virus budding assays for rVSV-wt, rVSV-D125A, and rVSV-wt + D125A were performed and quantified as described in (A). (C) Virus growth curves from cells infected with rVSV-wt (MOI = 1), rVSV-D125A (MOI = 10), or co-infected with rVSV-wt (MOI = 1) and rVSV-D125A (MOI = 10). (D) M-*skeleton* exchange assay. *Skeletons* from rVSV-wt (top panel) or rVSV-D125A (bottom panel) were incubated with soluble, in vitro translated, ^{35}S-methionine labeled Mwt or D125A. After incubation, the mixtures were centrifuged over a sucrose cushion to separate *skeletons* and associated M proteins (P; pellet) from unincorporated, soluble M (S; supernatant). (E) Depiction of the M-*skeleton* exchange assay results showing the inability of rVSV-wt *skeletons* to exchange with input M (green dots) versus the ability of the rVSV-D125A *skeletons* to incorporate the input M proteins. (For interpretation of the references to colour in this figure legend, the reader is referred to the web version of this article.)

experiments we infected BHK cells with rVSV-wt using a multiplicity of 1 and rVSV-D125A using a multiplicity of 10 to ensure that any effects seen were not due to more extensive or rapid replication of rVSV-wt. Analysis of virus growth indicated that virus replication and final virus titers produced by the singly infected cells were not affected by synchronization with NH_4Cl (compare Figs. 2A and 3C), but that co-infection resulted in a partial rescue of the amount of virus produced (Fig. 3C). Quantification of N protein expression at 4 hpi in Fig. 3B showed that the amount of N protein released (viral pellet (VP)/cell extract (CE) from rVSV-wt infected cells was approximately 16% of total N, while the D125A infected cells released only 0.9%. Co-infection increased the amount of virus released to 8% of total cellular N protein, which suggests that the D125A mutant is not dominant-negative for virion assembly or release.

rVSV-D125A M-RNP skeletons exchange more efficiently with input M proteins

To determine if the decrease in virus release seen with the D125A mutant could be due to reduced interaction of the mutant M protein with RNPs and consequently result in inefficient RNP condensation and budding, we performed a *skeleton*-M protein exchange assay, which was based on an assay described previously (Flood and Lyles, 1999) with modifications. The modified assay measures the ability of labeled M protein to bind with unlabeled *skeletons* released from the viral envelope versus the previously described assay (Flood and Lyles, 1999) in which most of the M protein was removed from purified *skeletons* before examining reassociation or exchange of M with RNPs at different NaCl concentrations. Our modification tests the ability of the *skeleton* to exchange M proteins as opposed to binding of M to RNPs. Using this assay to examine the efficiency of D125A RNP condensation of *skeletons*, we took 10, 50, or 100 μg of purified rVSV-wt or rVSV-D125A and detergent solubilized in the presence of ^{35}S-Met labeled wt or D125A M proteins that had been synthesized in an in vitro translation system. *Skeletons* with newly bound labeled M proteins were then separated from soluble M by ultracentrifugation and the pellets and supernatants were analyzed by SDS-PAGE and fluorography. We observed that the rVSV-wt *skeletons* did not incorporate any input ^{35}S-Met labeled M protein even with the highest amount of virus used where more *skeletons* would be available to exchange with input M (Fig. 3D, Wt *skeleton*). In contrast, the D125A *skeletons* exchanged with each of the input labeled M proteins regardless of the amount of *skeletons* in the assay (Fig. 3D, D125A *skeleton*). These data suggested that the D125A M protein was less tightly associated with *skeletons* isolated from rVSV-D125A virions. Alternatively, the D125A-*skeletons* may be less condensed and therefore could allow more binding of exogenous M protein as depicted in Fig. 3E.

rVSV loop mutants have reduced protein synthesis at late times post-infection

Previously it was shown that rVSV-ΦM had a defect in viral protein synthesis (Connor et al., 2006). To determine if our rVSV-M loop mutants had a similar translation defective phenotype we infected BHK cells at an MOI of 10 and pulse-labeled the cells with ^{35}S-Met for 10 min at 6 hpi since this was the time point which Connor et. al. began to see viral protein translation defects. Whole cell lysates were prepared and analyzed by SDS-PAGE and radiofluorography, and the relative amounts of N and P proteins synthesized during the 10 min pulse were quantified using phosphorimager analysis. Quantification of viral protein synthesis compared to rVSV-wt indicated that rVSV-D125A had the most pronounced reduction in viral protein translation at 6 hpi when compared to the other M loop mutants (data not shown).

To examine the difference in viral protein synthesis between rVSV-wt and rVSV-D125A infected cells in more detail, BHK cells were pulse-labeled with ^{35}S-Met for 10 min at 2, 4, 6, and 8 hpi and analyzed as described above. The synthesis of viral and host cellular proteins was similar for the two viruses at 2 and 4 hpi, and the characteristic inhibition of cellular protein synthesis was seen for both viruses at 4 hpi. However, by 6 and 8 hpi there was a dramatic reduction in viral protein synthesis for the rVSV-D125A mutant. Quantification of viral protein synthesis at 8 hpi from rVSV-D125A infected cells showed an 82% reduction compared to rVSV-wt levels (Fig. 4A, lane 8, and B). Based on the lack of other proteins that were detected in the cell lysate at 8 hpi, it appears that there was very little viral or cellular protein synthesis occurring in the rVSV-D125A

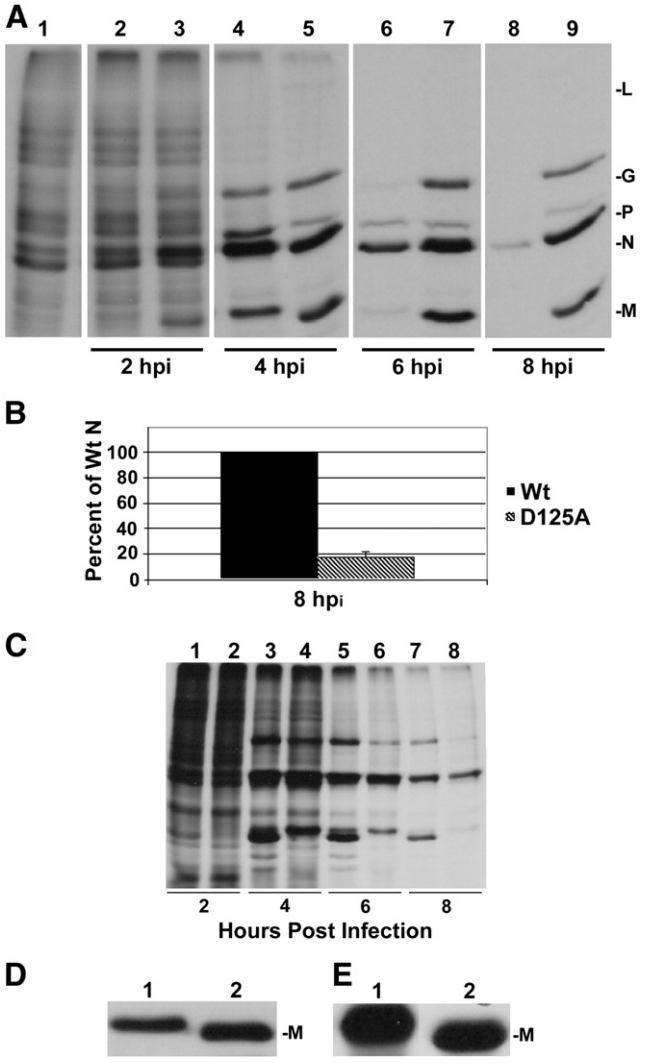

Fig. 4. Reduced viral protein synthesis at late times post-infection in rVSV-D125A infected cells. (A) BHK-21 cells were mock infected (lane 1) or infected with rVSV-wt (lanes 3, 5, 7, and 9), or rVSV-D125A (lanes 2, 4, 6, and 8) and then pulse-labeled with ^{35}S-methionine at the times indicated. Cell lysates were prepared immediately after the pulse and analyzed directly by SDS-PAGE. The slower migration of the D125A protein is due to the C-terminal Lumio tag. (B) Quantitation of the amount of N protein labeled during the 10 min pulse at 8 hpi in wt and D125A infected cells. Percent of wt N is shown for experiments done in triplicate (error bars; standard deviation). (C) HeLa cells were infected with rVSV-wt (lanes 1, 3, 5, and 7) or rVSV-D125A (lanes 2, 4, 6, and 8) at an MOI of 10 and pulse-labeled with ^{35}S-methionine at increasing times post-infection and cell lysates examined by SDS-PAGE and fluorography. (D) ^{35}S-methionine pulsed BHK-21 cell lysates from cells transiently expressing D125A (lane 1) or Mwt (lane 2) using the vaccinia-T7 expression system. (E) ^{35}S-methionine labeled D125A (lane 1) and Mwt (lane 2) protein synthesized in rabbit reticulolysates from an in vitro transcription-translation reaction.

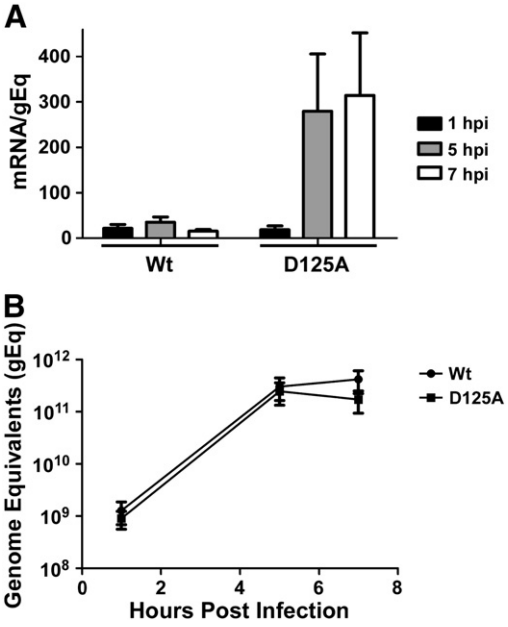

Fig. 5. Relative levels of VSV mRNA synthesis in rVSV-infected cells. (A) Quantitative RT-PCR was used to quantify the relative amount of phosphoprotein (P) mRNA to viral genomic RNA (mRNA/gEq) in rVSV-wt (Wt) and rVSV-D125A (D125A) infected cells at 1, 5, and 7 hpi. (B) qRT-PCR shows that the amount of genomic RNA for each virus was similar in these experiments ($n=3$; error bars, standard deviation).

infected cells at this time point. This reduction in VSV protein synthesis at later times post-infection was also seen in HeLa cells (Fig. 4C) and the timing of the reduction was similar. The lack of protein labeling was not due to an inhibition of ^{35}S-Met uptake by the cells as the intracellular pools of soluble ^{35}S-Met were similar for wt- and D125A-infected cells (data not shown).

Transient or in vitro expression of the D125A mutant does not affect protein synthesis

To determine if reduced VSV protein synthesis was induced by the mutant M protein alone we transiently expressed the D125A or wild-type M (Mwt) proteins in cells using the vaccinia-T7 system, and examined the relative amount of M protein made after a 10 min pulse labeling with ^{35}S-Met at 18 h post-transfection (Fig. 4D). We also analyzed protein expression using an in vitro transcription and translation system and compared the amount of protein synthesized by the D125A mutant and Mwt by SDS-PAGE, fluorography, and phosphorimaging (Fig. 4E). There was no difference in the amount of M protein synthesized in the absence of a VSV infection (Fig. 4D and E) in contrast to what was observed at 8 hpi (Fig. 4A–C). These data indicated that the reduced viral protein synthesis observed is not due solely to expression of the D125A mutant, but occurs in the context of VSV infection, perhaps requiring other viral proteins or products.

Viral mRNA is not the limiting factor in the rVSV-D125A protein synthesis defect

To determine if the reduced levels of viral protein synthesis seen in rVSV-D125A infected cells were due to a reduction in viral mRNA, we performed quantitative RT-PCR (qRT-PCR) on RNA isolated from infected BHK cells at varying times post-infection. Cells were infected with rVSV-wt or rVSV-D125A at an MOI of 10, RNA was isolated at 1, 5 or 7 hpi, and the amounts of VSV genomic RNA and P mRNA were determined. We found that the ratio of P mRNA to genomic RNA was ~8-fold higher at 5 hpi and 20-fold higher at 7 hpi in rVSV-D125A infected cells when compared to rVSV-wt infected cells (Fig. 5A). Importantly, the amounts of genomic RNA present for the two viruses were not significantly different (Fig. 5B). These results indicate that decreased mRNA synthesis was not responsible for the reduced viral protein synthesis seen with the rVSV-D125A mutant. In fact, there was significantly more viral mRNA per genome in the mutant infected cells than in rVSV-wt infected cells.

Co-infection with rVSV-wt partially rescues the protein translation defect

To determine if rVSV-wt infection could rescue the protein synthesis defect of the rVSV-D125A mutant, we co-infected BHK cells with rVSV-wt and rVSV-D125A using the synchronized fusion method as described for Fig. 3. Cells were either singly infected with rVSV-wt (MOI 1), doubly infected with rVSV-wt (MOI 1) and rVSV-D125A (MOI 10), or singly infected with rVSV-D125A (MOI 10). At 9 hpi cells were pulse-labeled with ^{35}S-Met and analyzed by SDS-PAGE, radiofluorography, and phosphorimaging (Fig. 6). We found that co-infection could partially rescue the protein synthesis defect (Fig. 6A, compare lanes 2 and 3), increasing the amount of viral proteins made 3-fold from approximately 20–60% of the amount made in rVSV-wt infected cells (Fig. 6B). These data indicate that D125A does not have a dominant-negative effect on translation.

rVSV-D125A infection does not reduce cap-independent protein synthesis

To determine if cap-independent protein synthesis was affected in rVSV-D125A infected cells, we transfected BSR cells constitutively expressing T7 polymerase with a plasmid that has a T7 promoter driving expression of the luciferase gene with an encephalomyocarditis virus (EMCV) IRES leader. At 18 h p.t., cells were mock infected,

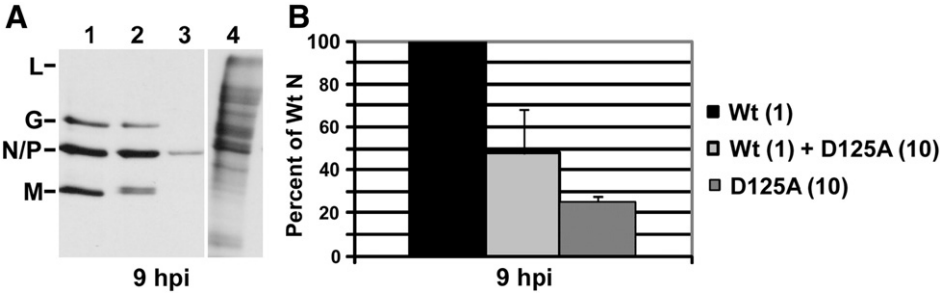

Fig. 6. Co-infection with rVSV-wt and rVSV-D125A partially rescues protein translation defect. (A) Viral protein synthesis in BHK-21 cells was examined in cells infected with rVSV-wt (MOI 1; lane 1), co-infected with wt and D125A (MOI 1 and 10, respectively; lane 2), or infected with rVSV-D125A (MOI 10; lane 3) by ^{35}S-methionine pulse labeling at 9 hpi. Lane 4 is from mock-infected cells. Cell lysates were analyzed by SDS-PAGE and radiofluorography. (B) Quantitation of protein synthesis by phosphorimager analysis ($n=3$; error bars, standard deviation).

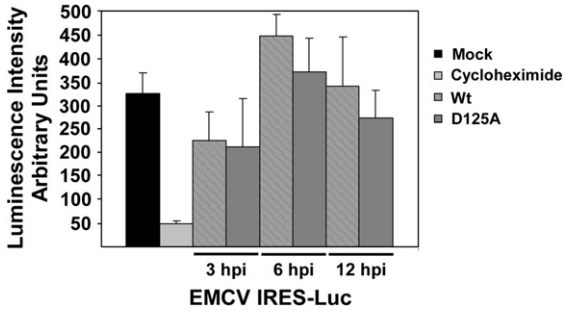

Fig. 7. EMCV/IRES-driven expression of luciferase is not affected in rVSV-D125A infected BSR cells. BSR cells constitutively expressing T7 RNA polymerase were transfected with a plasmid that expresses IRES-luciferase from a T7 promoter. Eighteen hours post-transfection the cells were mock treated/infected, treated with cycloheximide, or infected with rVSV-wt (Wt) or rVSV-D125A (D125A). Luciferase activity was measured 6 h after cycloheximide treatment, or 3, 6, or 12 hpi ($n=3$; error bars, standard deviation).

treated with cycloheximide, or infected with rVSV-wt or rVSV-D125A at an MOI of 10, and cell lysates were analyzed for luciferase activity at increasing times post-infection. The results (Fig. 7) showed a slight reduction in luciferase activity in the rVSV-D125A infected cells compared to wt-infected cells, but this difference was not statistically significant, indicating that the mechanism responsible for the reduced protein synthesis seen at increasing times post-infection in rVSV-D125A infected cells primarily affected synthesis of proteins produced by a cap-dependent mechanism.

Discussion

The initial crystallization of the VSV-Ind M protein was made possible by proteolytic cleavage of an exposed loop (amino acids 121–128) that prevented M self-association (Barge et al., 1996; Gaudier et al., 2001, 2002; Gaudin et al., 1995, 1997). The self-association of uncleaved M protein can be prevented by high salt (Gaudin et al., 1995), which also causes the release of M from *skeletons* and subsequent RNP decondensation (Newcomb et al., 1982). These observations suggested that the exposed loop may be involved in virus assembly, specifically RNP condensation into *skeletons*. Previously, others reported that mutations of amino acids 121–124 within the loop resulted in a minor assembly defect, but the major effect of the mutations was an unexpected reduction in viral protein synthesis (Connor et al., 2006). Here, we report that mutations in the conserved LXD motif (amino acids 123–125) within the loop region have two major effects on VSV biology, namely, an effect on virus assembly and an effect on viral protein synthesis.

Transient expression of a series of M protein loop mutants revealed no discernable differences in the cellular distribution or budding activity for any of the mutants when compared to Mwt; however, we could only recover rVSVs encoding three of the eight mutants despite multiple attempts ($n=6$ per virus). These data indicated that the size of the loop and specific residues within the loop were essential for M protein function required for virus recovery. For the rVSV mutants that were recovered, the viruses displayed reduced growth kinetics (Figs. 2A and 3C) that correlated with reduced virus budding (Fig. 3A and B) compared to rVSV-wt. These data suggested the mutations in the loop of M affected the efficiency of VSV assembly and we propose that this is due to inefficient condensation of RNPs into *skeletons*. Additional observations supporting this hypothesis include the high viral mRNA to genome ratio found in rVSV-D125A infected cells (Fig. 5) and the increased level of M protein exchange seen with rVSV-D125A *skeletons* (Fig. 3D). The high viral mRNA to genome ratio suggested that the genomes in the rVSV-D125A cells were less condensed than the rVSV-wt genomes since M condensation of the RNP is thought to inhibit transcription (Carroll and Wagner, 1979; Pal et al., 1985). This is supported by the exchange of M protein with rVSV-D125A *skeletons*, but not with rVSV-wt *skeletons*, which we propose reflects the less condensed nature of D125A *skeletons*. These data, together with the crystal structure of VSV-NJ M oligomers which shows M–M interactions involving amino acids 120–128 (Graham et al., 2008), and the cryo-EM model of VSV virions where amino acids 120–128 are in contact 4 of the M-hub which is important in setting the vertical spacing of the M protein helix (Ge et al., 2010), suggest that the LXD motif is important for efficient condensation of VSV RNPs by M into *skeletons*.

In addition to the effects on virus assembly, some of the mutations in the loop region also inhibited viral protein expression, similar to that reported by others for a different set of loop mutations (Connor et al., 2006). We quantified the amount of VSV mRNA synthesized in rVSV-wt and D125A infected cells and found the reduced level of VSV protein synthesis was not due to reduced viral mRNA production. We also found this was not due to differences in PKR-mediated phosphorylation of eIF2α, nor to enhanced RNAse L activation, and we detected no difference in cleavage of pro-caspase 3 to caspase 3, or conversion of LC3 to LC3B in rVSV-D125A versus rVSV-wt infected cells (data not shown). These data suggested the reduced protein synthesis was not due to an enhanced host response to rVSV-D125A infection, but a more thorough examination of each of these processes individually needs to be conducted before they can be completely ruled out as having no effect on VSV protein synthesis in rVSV-D125A infected cells.

Recently, a new model was proposed for control of host and viral protein synthesis in VSV-infected cells (Connor and Lyles, 2002). This model proposes that alterations of the eIF4F cap-binding complex result in inhibition of host protein synthesis and the pre-existing host mRNAs are then shuttled to inactive mRNPs which in turn allows for newly made viral mRNA to be translated. A follow-up study showed that this effect was not specific to newly made VSV mRNAs but also occurred with a reporter expressed during VSV infection (Whitlow et al., 2008). These observations suggest that the time when mRNAs enter the translation machinery after VSV infection is critical for preferential translation and is not the result of cis-acting structural elements in the 5′ untranslated region (UTR) of VSV mRNA, as has also been suggested (Whitlow et al., 2006). Interestingly, the major effects of alterations to the eIF4F cap-binding complex on host protein translation during VSV infection occur between 4 and 8 hpi (Black et al., 1994; Connor et al., 2006; Whitlow et al., 2008), which was the time post-infection that we observed a reduction in both viral and host protein synthesis in the mutant infected cells (Fig. 4A and C). Therefore, the dramatic reduction in VSV protein synthesis seen in this study may reflect the inability of the D125A mutant to positively regulate viral protein synthesis beginning ~4 hpi. Whether this positive translation regulation by Mwt at later times post-infection is due to its ability to support the initiation of translation using altered eIF4F cap-binding complexes or is due to some other mechanism, it is clear that VSV M protein contributes to regulation of protein translation after ~4 hpi and that for VSV-Ind M, amino acids 121–125 are important for this effect, with the D125 residue being critical.

Eukaryotic protein translation initiation is a complex process that requires many co-factors, but cap-independent translation of mRNA from picornaviruses, such as *encephalomyocarditis virus* (EMCV), requires a smaller number of initiation factors when compared to those required for cap-dependent translation initiation (Pestova et al., 2001). EMCV mRNA contains a 5′ UTR that has an internal ribosome entry site (IRES) (Hellen and Wimmer, 1995; Jang et al., 1990) and initiation of translation from the EMCV IRES in vitro only requires ATP, eIF2, eIF3, eIF4A or eIF4F, and the central portion of eIF4G (Pestova et al., 2001). Although it is still possible that the reduction in viral

protein synthesis we observed with the rVSV-D125A mutant was due to an untested host response induced by inefficient virus assembly, our results suggest that the effect was more likely due to the inability of the M loop mutant proteins to positively regulate VSV translation after 4 hpi. Indeed, we found that EMCV IRES-driven luciferase expression was not significantly affected by rVSV-D125A infection. In fact, there was a slight increase in luciferase expression at 6 hpi in rVSV-D125A infected cells when compared to mock-infected cells (Fig. 7) where newly made mRNA should be preferentially translated (Whitlow et al., 2008). These data suggest that a cap-dependent translation initiation factor is involved in the protein synthesis effect observed during rVSV-M loop mutant infections. One candidate factor is eIF4E since it is the only major initiation factor that is not required for EMCV IRES protein translation initiation but it is required for cap-dependent β-globin mRNA translation (Pestova et al., 2001). Previously it was proposed that dephosphorylation of the eIF4E binding protein 4E-BP1 contributes to the reduction in host protein translation during VSV infection (Connor and Lyles, 2002). The data presented here, together with that published by others (Black et al., 1994; Connor and Lyles, 2002, 2005; Connor et al., 2006; Whitlow et al., 2006, 2008), suggests that M protein may support VSV translation at later times post-infection by compensating for the alteration of the eIF4F cap-binding complex The hypothesis that M may be able to substitute for or enhance eIF4E activity is intriguing since the two proteins are similar in size, both have an unstructured N-terminus, and have similar crystal structures (Brown et al., 2007; Gaudier et al., 2002). Whether the assembly and translational phenotypes of the LXD mutants described here can be separated genetically will require additional investigation. Alternatively, the LXD motif could be the first dual function motif of the M protein described to date.

Materials and methods

Plasmid design and construction

Construction of the cDNAs containing the loop mutations in M was accomplished using an overlap PCR strategy with mutagenic primers and pBluescript (pBS) M-Lumio (Mire et al., 2009) as the template. Complementary mutagenic primers (sequences available upon request) were used with either a 5′ forward primer (CEM 1) or a 3′ reverse primer (T3) to generate the mutants: Δ Loop, 2X Loop, A Loop, D Loop, D125A, D125E, L123A, and L123S. A second round of PCR amplification, with the overlapping 5′ and 3′ fragments used as the templates, together with the two outside primers (CEM 1 and T3) were used to create the desired mutations in the M-Lumio gene. The PCR products were gel purified, digested with *AscI* and *EagI*, gel purified again, and ligated into pBS-SK-ΦT (Stillman et al., 1995) cut with the same enzymes.

Generation of full-length VSV cDNAs encoding M loop mutants

Creation of the full-length VSV genomes with M loop mutants was accomplished by separately cloning each sequence into pVSV-ΔM-PL, which encodes a VSV anti-genome that has a multiple cloning site in the place of the M protein coding sequence (Jayakar et al., 2000). For each construct the plasmids were digested with *Asc*I and *Eag*I, and the ΔM vector and M loop mutant fragments were gel purified and ligated by two way ligation to create pVSV-"Loop Mutant" (e.g., pVSV-D125A, etc.).

Recovery and characterization of recombinant VSV (rVSV)

Recombinant viruses were recovered using reverse genetics (Lawson et al., 1995) with some modifications as described previously (Jayakar et al., 2000). Single-step growth curves were performed by adsorbing virus to baby hamster kidney (BHK-21) cells in 35 mm plates at a multiplicity of infection (MOI) of 10 for 1 h while continually rocking. The inoculum was removed, the cells were washed 4x with serum-free Dulbecco's minimal Eagle's medium (DMEM) to remove unbound virus, DMEM containing 5% fetal bovine serum (FBS) was added, and the cells were placed at 37 °C. Every 2 h post-infection (hpi) a 5% aliquot of media was collected, replaced with the same volume of fresh media, and then virus titers were determined in duplicate by plaque assay on BHK-21 cells. Growth curves were performed in triplicate for each virus. Relative infectivity was assessed by Coomassie-blue staining after SDS-PAGE analysis of 1 x 10^7 PFU of rVSV.

TEM of rVSV

To confirm the morphology of rVSV, purified virus was resuspended in 10% sucrose 10 mM Tris–HCl [pH 8.0], 150 mM NaCl solution and placed on ice. To decrease the sucrose concentration, the virus preparations were then diluted 1:10 in dH_2O and prepared for transmission electron microscopy (TEM) after adsorbing virus to a carbon-coated grid by placing the grid on a drop of virus suspension, and negative staining with 2% phosphotungstic acid (PTA, pH 5.9).

Transient expression of M loop mutants

BHK-21 cells at ~90% confluence on glass cover slips were infected with a modified vaccinia virus (vTF7-3) encoding T7 RNA polymerase (Fuerst et al., 1987) at MOI 5 for 1 h at 31 °C in SF-DMEM. The inoculum was removed and the cells were transfected with 5 μg of pBS-MΦT (wild-type; Indiana) or pBS-(Loop Mutant) using 20 μl TransfectACE in SF-DMEM (Rose et al., 1991). Five hours post-transfection (p.t.) the transfection mix was removed and replaced with 5% FBS DMEM containing antibiotics (100 U/ml streptomycin and penicillin), and 18 h p.t. the cells were fixed and processed for immunofluorescence or were used in a budding assay as described below.

Immunofluorescence (IF) staining and confocal microscopy

Cells either transiently expressing M proteins from plasmids or infected with rVSV were washed twice with phosphate-buffered saline (PBS) and then fixed for 15 min with 3% paraformaldehyde (PFA) in PBS at room temperature (r.t.). The fix solution was then removed and the cells washed twice with PBS containing 10 mM glycine and 0.05% sodium azide (PBS–glycine), and then permeabilized with 1% Triton X-100 in PBS–glycine at r.t. for 1 min. After permeabilization, the cells were washed twice with PBS–glycine and then stained for M protein using an anti-M monoclonal antibody (mAb 23H12) conjugated to Alexa-488. The distribution of the M proteins was examined using laser scanning confocal microscopy (Zeiss LSM 510). Optical slices of 1 μm were captured using 488 nm laser excitation.

Budding assays

Cells transiently expressing the indicated M protein were washed twice with methionine-free SF-DMEM and then incubated in this media for 15 min to deplete the intracellular methionine pools at 5 h p.t. After depletion, a medium composed of 1 part 5% FBS DMEM to 9 parts methionine-free media and supplemented with 50 μCi of ^{35}S-Methionine (Met) Express Protein Labeling Mix (Perkin-Elmer) per ml was added and 18 h later media and cells were collected separately and processed for immunoprecipitation (IP). The media were centrifuged at 170 × *g* for 10 min to remove dislodged cells and the supernatant was placed on ice after addition of 200 U of aprotinin (U.S. Biochemicals). The supernatant was made to 50 mM Tris–HCl,

150 mM NaCl, 0.1% NP-40, 1 mM EDTA, 20 mM NaN_3, 0.3% SDS, and radiolabeled M proteins were immunoprecipitated with M mAb (23H12) overnight at 4^0C. Cell extracts were prepared by washing the cells twice with PBS and then lysing with 800 µl of Detergent Solution (10 mM Tris–HCl [pH 7.4], 66 mM EDTA, 0.4% sodium deoxycholate, 1% Triton X-100, 0.05% NaN_3) containing 200 U/ml of aprotinin for 5 min at r.t. on a rocker. The cell extract was collected, nuclei and insoluble material were removed by centrifugation at 10,000×*g* for 5 min and a 200 µl aliquot of the cell extract was made to 0.3% SDS and immunoprecipitated with M mAb (23H12) overnight at 4 °C. One-quarter of the radiolabeled M proteins in the cell extracts were compared to the amount released into the supernatant by SDS polyacrylamide gel electrophoresis (PAGE) on a 9% polyacrylamide gel and visualized by radiofluorography.

^{35}S-methionine pulse labeling of rVSV-infected cells

BHK-21 and HeLa cells were infected with rVSV at an MOI of 10. At increasing times post-infection the cells were starved of methionine for 10 min and then a ^{35}S-Met labeling mix at 50 µCi/ml was added to the cells for 10 min. Cell extracts were prepared by washing the cells twice with PBS and then lysing with 400 µl of Detergent Solution containing 200 U/ml of aprotinin for 5 min at r.t. on a rocker. The nuclei and insoluble material were removed by centrifugation at 10,000×*g* for 5 min and 5% of the cell extract was analyzed by SDS-PAGE radiofluorography and quantified by phosphorimaging using a STORM (Molecular Dynamics) scanner.

rVSV budding assay

BHK-21 cells were infected with rVSV at an MOI of 10. At 3 hpi, cells were starved of methionine for 10 min and then an ^{35}S-Met labeling mix at 50 µCi/ml was added to the cells for 1 h. The supernatant was then collected and virus was isolated from the supernatant by ultracentrifugation (35 min, 45 K rpm, Sorvall, AH-650) over a 20% sucrose–TN (10 mM Tris–HCl [pH 8.0], 150 mM NaCl) cushion. Also, cell extracts were prepared by washing the cells twice with PBS and then lysing with 400 µl of Detergent Solution containing 200 U/ml of aprotinin for 5 min at r.t. on a rocker. The nuclei and insoluble material were removed by centrifugation at 10,000×*g* for 5 min. The whole viral pellet and 5% of the cell extract were analyzed by SDS-PAGE radiofluorography and quantified by phosphorimaging using a STORM scanner.

Synchronized fusion co-infection assay

To prevent the acidification of endosomes and synchronize fusion of virions with endosomal membranes we used the lysosomotropic reagent NH_4Cl as described previously (Mire et al., 2010; Rigaut et al., 1991) with some modifications. BHK-21 cells were washed twice with PBS and then washed twice with PBS containing 100 mM NH_4Cl. rVSV (MOI 1), rVSV-D125A (MOI 10), or rVSV-wt (MOI 1) and rVSV-D125A (MOI 10) were adsorbed in SF-DMEM containing 100 mM NH_4Cl for 90 min. After adsorption the cells were washed with PBS four times to remove the NH_4Cl and protein synthesis or virus budding was examined by ^{35}S-Met pulse labeling as described above.

RNP exchange assay

^{35}S-Met labeled Mwt or M D125A mutant protein was made from plasmids in a TNT T7 in vitro transcription and translation reaction (# L4610, Promega) in the presence of ^{35}S-methionine labeling mix (# AG1594, GE Healthcare). Five microliters of either translation reaction was added to 10, 50, or 100 µg of solubilized rVSV-wt or rVSV-D125A in TN (Tris–HCl (pH 8.0), 150 mM NaCl) buffer. The mixtures were placed on ice for 10 min and then the *skeletons* and supernatants were separated by ultracentrifugation (35 min, 45 K rpm, Sorvall, AH-650) over a 20% sucrose–TN cushion. Pellets and TCA precipitated supernatants were then analyzed by SDS-PAGE radiofluorography.

qRT-PCR analysis

To rule out viral mRNA as the limiting factor in the reduction in protein synthesis during infection, real-time RT-PCR was performed on BHK-21 cells infected with rVSV at an MOI of 10. At increasing times post-infection cell lysates were collected in Trizol reagent (# 15596–018, Invitrogen) and total RNA was extracted. Reverse transcription was performed using a primer (MR Nest) on a known amount of genomes (from 10^1 to 10^{13}) to produce a standardized genomic curve for RT-PCR. Reverse transcription was also performed on total RNA extracted from cells using a poly dT primer for mRNA and a primer (MR Nest) that annealed to the intergenic region between M and G for genomes. RT-PCR was then performed and RNA was quantified using SYBR Green for genomes (primers CEM 2 and MR Nest) and P mRNA (P82F and P-210-REV) in a DNA Engine Opticon system and software (MJ Research/BioRad).

Luciferase assay

BSR-T7 cells (BHKs constitutively expressing T7 RNA polymerase, (Buchholz et al., 1999)) were transfected with 5 µg of a plasmid that expressed luciferase with an internal ribosome entry site (pEMCV/IRES-Luc) and 18 h p.t. the cells were mock infected/treated, treated with cycloheximide (10 µg/ml), or infected with rVSV-wt or rVSV-D125A at an MOI of 10. Mock and cycloheximide treated cell lysates were assessed for luciferase activity at 6 h post-treatment and luciferase activity was measured at increasing times post-infection in infected cells as described above.

Acknowledgments

We thank Fabio Re (UTHSC) for the pIFNβ-Luc plasmid and Charles Russell (St. Jude Children's Research Hospital) for the BSR-T7 cells. We also thank Carolyn Matthews for technical assistance and for management of the LSCM facility, which was made available through NCRR grant RR13725 to M.A.W.

References

Ahmed, M., Lyles, D.S., 1998. Effect of vesicular stomatitis virus matrix protein on transcription directed by host RNA polymerases I, II, and III. J. Virol. 72 (10), 8413–8419.

Ahmed, M., McKenzie, M.O., Puckett, S., Hojnacki, M., Poliquin, L., Lyles, D.S., 2003. Ability of the matrix protein of vesicular stomatitis virus to suppress beta interferon gene expression is genetically correlated with the inhibition of host RNA and protein synthesis. J. Virol. 77 (8), 4646–4657.

Barge, A., Gagnon, J., Chaffotte, A., Timmins, P., Langowski, J., Ruigrok, R.W., Gaudin, Y., 1996. Rod-like shape of vesicular stomatitis virus matrix protein. Virology 219 (2), 465–470.

Black, B.L., Brewer, G., Lyles, D.S., 1994. Effect of vesicular stomatitis virus matrix protein on host-directed translation in vivo. J. Virol. 68, 555–560.

Brown, E.L., Lyles, D.S., 2003a. A novel method for analysis of membrane microdomains: vesicular stomatitis virus glycoprotein microdomains change in size during infection, and those outside of budding sites resemble sites of virus budding. Virology 310 (2), 343–358.

Brown, E.L., Lyles, D.S., 2003b. Organization of the vesicular stomatitis virus glycoprotein into membrane microdomains occurs independently of intracellular viral components. J. Virol. 77 (7), 3985–3992.

Brown, C.J., McNae, I., Fischer, P.M., Walkinshaw, M.D., 2007. Crystallographic and mass spectrometric characterisation of eIF4E with N7-alkylated cap derivatives. J. Mol. Biol. 372 (1), 7–15.

Buchholz, U.J., Finke, S., Conzelmann, K.K., 1999. Generation of bovine respiratory syncytial virus (BRSV) from cDNA: BRSV NS2 is not essential for virus replication in tissue culture, and the human RSV leader region acts as a functional BRSV genome promoter. J. Virol. 73 (1), 251–259.

Carroll, A.R., Wagner, R.R., 1979. Role of the membrane (M) protein in endogenous inhibition of in vitro transcription of vesicular stomatitis virus. J. Virol. 29, 134–142.

Chong, L.D., Rose, J.K., 1994. Interactions of normal and mutant vesicular stomatitis virus matrix proteins with the plasma membrane and nucleocapsids. J. Virol. 68, 441–447.
Connor, J.H., Lyles, D.S., 2002. Vesicular stomatitis virus infection alters the eIF4F translation initiation complex and causes dephosphorylation of the eIF4E binding protein 4E-BP1. J. Virol. 76 (20), 10177–10187.
Connor, J.H., Lyles, D.S., 2005. Inhibition of host and viral translation during vesicular stomatitis virus infection. eIF2 is responsible for the inhibition of viral but not host translation. J. Biol. Chem. 280 (14), 13512–13519.
Connor, J.H., McKenzie, M.O., Lyles, D.S., 2006. Role of residues 121 to 124 of vesicular stomatitis virus matrix protein in virus assembly and virus-host interaction. J. Virol. 80 (8), 3701–3711.
Faria, P.A., Chakraborty, P., Levay, A., Barber, G.N., Ezelle, H.J., Enninga, J., Arana, C., van Deursen, J., Fontoura, B.M., 2005. VSV disrupts the Rae1/mrnp41 mRNA nuclear export pathway. Mol. Cell 17 (1), 93–102.
Flood, E.A., Lyles, D.S., 1999. Assembly of nucleocapsids with cytosolic and membrane-derived matrix proteins of vesicular stomatitis virus. Virology 261 (2), 295–308.
Fuerst, T.R., Earl, P.L., Moss, B., 1987. Use of a hybrid vaccinia virus-T7 RNA polymerase system for expression of target genes. Mol. Cell. Biol. 7, 2538–2544.
Gaudier, M., Gaudin, Y., Knossow, M., 2001. Cleavage of vesicular stomatitis virus matrix protein prevents self-association and leads to crystallization. Virology 288 (2), 308–314.
Gaudier, M., Gaudin, Y., Knossow, M., 2002. Crystal structure of vesicular stomatitis virus matrix protein. EMBO J. 21 (12), 2886–2892.
Gaudin, Y., Barge, A., Ebel, C., Ruigrok, R.W.H., 1995. Aggregation of VSV M protein is reversible and mediated by nucleation sites: implication for viral assembly. Virology 206, 28–37.
Gaudin, Y., Sturgis, J., Doumith, M., Barge, A., Robert, B., Ruigrok, R.W., 1997. Conformational flexibility and polymerization of vesicular stomatitis virus matrix protein. J. Mol. Biol. 274 (5), 816–825.
Ge, P., Tsao, J., Schein, S., Green, T.J., Luo, M., Zhou, Z.H., 2010. Cryo-EM model of the bullet-shaped vesicular stomatitis virus. Science 327 (5966), 689–693.
Graham, S.C., Assenberg, R., Delmas, O., Verma, A., Gholami, A., Talbi, C., Owens, R.J., Stuart, D.I., Grimes, J.M., Bourhy, H., 2008. Rhabdovirus matrix protein structures reveal a novel mode of self-association. PLoS Pathog. 4 (12), e1000251.
Harty, R.N., Brown, M.E., McGettigan, J.P., Wang, G., Jayakar, H.R., Huibregtse, J.M., Whitt, M.A., Schnell, M.J., 2001. Rhabdoviruses and the cellular ubiquitin–proteasome system: a budding interaction. J. Virol. 75 (22), 10623–10629.
Hellen, C.U., Wimmer, E., 1995. Translation of encephalomyocarditis virus RNA by internal ribosomal entry. Curr. Top. Microbiol. Immunol. 203, 31–63.
Jang, S.K., Pestova, T.V., Hellen, C.U., Witherell, G.W., Wimmer, E., 1990. Cap-independent translation of picornavirus RNAs: structure and function of the internal ribosomal entry site. Enzyme 44 (1–4), 292–309.
Jayakar, H.R., Murti, K.G., Whitt, M.A., 2000. Mutations in the PPPY motif of vesicular stomatitis virus matrix protein reduce virus budding by inhibiting a late step in virion release. J. Virol. 74 (21), 9818–9827.
Lawson, N.D., Stillman, E.A., Whitt, M.A., Rose, J.K., 1995. Recombinant vesicular stomatitis viruses from DNA. Proc. Natl. Acad. Sci. U. S. A. 92 (10), 4477–4481.
Lyles, D.S., McKenzie, M.O., Daptur, P.E., Grant, K.W., Jerome, W.G., 1996. Complementation of M gene mutants of vesicular stomatitis virus by plasmid-derived M protein converts spherical extracellular particles into native bullet shapes. Virology 217, 76–87.
Mebatsion, T., Weiland, F., Conzelmann, K.K., 1999. Matrix protein of rabies virus is responsible for the assembly and budding of bullet-shaped particles and interacts with the transmembrane spike glycoprotein G. J. Virol. 73 (1), 242–250.
Mire, C.E., Dube, D., Delos, S.E., White, J.M., Whitt, M.A., 2009. Glycoprotein-dependent acidification of vesicular stomatitis virus enhances release of matrix protein. J. Virol. 83 (23), 12139–12150.
Mire, C.E., White, J.M., Whitt, M.A., 2010. A spatio-temporal analysis of matrix protein and nucleocapsid trafficking during vesicular stomatitis virus uncoating. PLoS Pathog. 6 (7), e1000994.
Newcomb, W.W., Brown, J.C., 1981. Role of the vesicular stomatitis virus matrix protein in maintaining the viral nucleocapsid in the condensed form found in native virions. J. Virol. 39, 295–299.
Newcomb, W.W., Tobin, G.J., McGowan, J.J., Brown, J.C., 1982. In vitro reassembly of vesicular stomatitis virus skeletons. J. Virol. 41 (3), 1055–1062.
Pal, R., Grinnell, B.W., Snyder, R.M., Wagner, R.R., 1985. Regulation of viral transcription by the matrix protein of vesicular stomatitis virus probed by monoclonal antibodies and temperature-sensitive mutants. J. Virol. 56 (2), 386–394.
Pestova, T.V., Kolupaeva, V.G., Lomakin, I.B., Pilipenko, E.V., Shatsky, I.N., Agol, V.I., Hellen, C.U., 2001. Molecular mechanisms of translation initiation in eukaryotes. Proc. Natl. Acad. Sci. 98 (13), 7029–7036.
Petersen, J.M., Her, L.S., Varvel, V., Lund, E., Dahlberg, J.E., 2000. The matrix protein of vesicular stomatitis virus inhibits nucleocytoplasmic transport when it is in the nucleus and associated with nuclear pore complexes. Mol. Cell. Biol. 20 (22), 8590–8601.
Rigaut, K.D., Birk, D.E., Lenard, J., 1991. Intracellular distribution of input vesicular stomatitis virus proteins after uncoating. J. Virol. 65, 2622–2628.
Rose, J.K., Buonocore, L., Whitt, M.A., 1991. A new cationic liposome reagent mediating nearly quantitative transfection of animal cells. Biotechniques 10, 520–525.
Stillman, E.A., Rose, J.K., Whitt, M.A., 1995. Replication and amplification of novel vesicular stomatitis virus minigenomes encoding viral structural proteins. J. Virol. 69, 2946–2953.
Swinteck, B.D., Lyles, D.S., 2008. Plasma membrane microdomains containing vesicular stomatitis virus M protein are separate from microdomains containing G protein and nucleocapsids. J. Virol. 82 (11), 5536–5547.
Whitlow, Z.W., Connor, J.H., Lyles, D.S., 2006. Preferential translation of vesicular stomatitis virus mRNAs is conferred by transcription from the viral genome. J. Virol. 80 (23), 11733–11742.
Whitlow, Z.W., Connor, J.H., Lyles, D.S., 2008. New mRNAs are preferentially translated during vesicular stomatitis virus infection. J. Virol. 82 (5), 2286–2294.